Non-contact Method for Producing Tactile Sensation Using Airborne Ultrasound

Takayuki Iwamoto, Mari Tatezono, and Hiroyuki Shinoda

Department of Information Physics and Computing
Graduate School of Information Science and Technology
The University of Tokyo
Eng.Bldg.6, 7-3-1, Hongo, Bunkyo Ward, Tokyo, Japan
{iwa,tatezono,shino}@alab.t.u-tokyo.ac.jp
http://www.alab.t.u-tokyo.ac.jp/~iwa

Abstract. This paper describes a new tactile device which produces stress fields in 3D space. Combined with 3D stereoscopic displays, this device is expected to provide high-fidelity tactile feedback for the interaction with 3D visual objects. The principle is based on a non-linear phenomenon of ultrasound, acoustic radiation pressure. We fabricated a prototype device to confirm the feasibility as a tactile display. The prototype consists of 91 airborne ultrasound transducers packed in the hexagonal arrangement, a 12 channel driving circuit, and a PC. The transducers which were in the same distance from the center of the transducer array were connected to form a 12 channel annular array. The measured total output force within the focal region was 0.8 gf. The spatial resolution was 20 mm. The prototype could produce sufficient vibrations up to 1 kHz.

Keywords: Tactile display, Airborne ultrasound, Acoustic radiation pressure.

1 Introduction

With the recent progress in the field of computer graphics, physical simulation and visual display technology, demands on haptic interaction techniques are increasing. Rodriguez et al. developed a 3D visual display system, Holovizio[1]. Holovizio has cameras to capture the motion of the user's hands and enables the user to handle 3D graphic objects. Another markerless 3D interaction system was proposed by Allard et al[2]. Their system GrImage synthesizes a 3D model of a real object from different points of view in real time. Hence, for example, the user of GrImage can interact with 3D graphic objects with the 3D models of their real hands captured and synthesized in real time. While these systems were designed to enable the users to handle 3D graphic objects with their bare hands, they do not provide tactile feedback. If tactile feedback is provided to the users' bare hands in free space, the usability of those systems will be highly improved.

There are two conventional strategies to provide tactile feedback in free space. One strategy is to attach tactile displays on the users' hands. Immersion developed CyberTouch[3] which features small vibrotactile stimulators on each finger

and the palm to interact with objects in a virtual world with tactile feedback. However, this strategy inherently degrades tactile feelings due to the contact between the skin and the device occurring even when there is no need to provide tactile sensation.

Another strategy is to control the position of tactile displays so that they contact with the skin only when tactile feedback is required. For instance, Sato et al.[4] proposed a multi-fingered master-slave robotic system featuring electrotactile displays on each finger of the master hand. The position of the electrotactile display is controlled so that it is in contact with the user's finger only when the slave robot grasps or touches objects. Major drawbacks of such systems are that they require bulky robot arms and complicated control method.

Air-jet is one possible candidate for providing haptic feedback in free space[5]. However, when it comes to producing fine texture sensation rather than kinetic feedback, as Drif pointed out[6], there are at least two major drawbacks. First, air-jet can not produce localized force due to diffusion. Second, it also suffers from limited bandwidth. In addition, even if multiple air-jet nozzles are used, the variation of the spatial distribution of the pressure is quite limited.

We have proposed a method for producing tactile sensation with ultrasound[7]. The previous prototypes utilized water as medium for sound propagation. By using airborne ultrasound, the method can be applied for tactile feedback to bare hands in free space with high spatial and temporal resolution. The spatial distribution of pressure is controlled by using wave field synthesis. In this paper, we show a prototype of the tactile display using airborne ultrasound and discuss the feasibility of the method.

2   Method

The method is based on a nonlinear phenomenon of ultrasound; acoustic radiation pressure. The acoustic radiation pressure P [Pa] is described as

$$P = \alpha E = \alpha \frac{w}{c} = \alpha \frac{p^2}{\rho c^2}, \tag{1}$$

where E [J/m^3] is the energy density of the ultrasound, w [W/m^2] is the sound power, c [m/s] is the sound speed, p [Pa] is the sound pressure of the ultrasound, and ρ [kg/m^3] is the density of the medium. α is a constant ranging from 1 to 2 depending on the reflection properties of the surface of the object. In case the surface of the object perfectly reflects the incident ultrasound, the value of α is 2, while if it absorbs the entire incident ultrasound, the value of α is 1. Eq. (1) suggests that the spatial distribution of the pressure can be controlled by using the wave field synthesis.

When the airborne ultrasound is applied on the surface of the skin, almost all the incident ultrasound is reflected. The characteristic acoustic impedance of the skin z_s and that of the air z_a are 1.52 and 0.0004 [Mkg/m$^2 \cdot$ s], respectively. (Note that for simplicity it is assumed that the characteristic acoustic impedance

of the skin is equal to that of the water.) In this case, the reflection ratio of the acoustic intensity R_I is calculated as,

$$R_I = \left| \frac{z_s - z_a}{z_s + z_a} \right|^2 \approx 0.9989. \tag{2}$$

Therefore, about 99.9% of the incident acoustic energy is reflected on the surface of the skin. There are two advantages induced by that fact. First, unlike the previous version of our ultrasound tactile display[7] which used water instead of air as medium, airborne ultrasound can be directly applied onto the skin. There is no need to place a clumsy ultrasound reflective film between the skin and medium. Another advantage is that the sound energy is effectively turned into the acoustic radiation pressure since the coefficient α in Eq. (1) is maximized under the perfect reflection condition.

We roughly estimated the total force produced with an array transducer. Suppose the array consists of ordinary airborne ultrasound transducers which are usually used for measuring the distance or detecting objects. A single transducer is capable of exerting 20 Pa of the sound pressure at the distance of 300 mm. If we assume the single transducer is regarded as a circular piston, the sound pressure along the center axis (z axis) is described as

$$p \doteqdot \rho c \frac{\pi}{\lambda} \frac{b^2}{z} |v_0| \qquad (z \gg b) \tag{3}$$

where λ, b, z, v_0 are the wavelength of the ultrasound, the radius of the transducer, the distance from the radiation surface, and the particle velocity at $z = 0$, respectively. The relationship between the sound power W [W] radiated from the transducer and v_0 is

$$W = S_0 \rho c r^A \frac{|v_0|^2}{2} \tag{4}$$

where S_0 and r^A are the area of the radiation surface for a single ultrasound transducer and the real part of the radiation impedance of the circular piston, respectively. If we assume $b = 5 \times 10^{-3}$ [m] and $\lambda = 8.5 \times 10^{-3}$ [m], then r^A becomes $r^A \doteqdot 1$. Using $z = 300 \times 10^{-3}$ [m], $|p| = 20$ [Pa], $\rho_0 = 1.2$ [kg/m³], $c = 340$ [m/s], from Eqs. 3 and 4, the sound power produced with a single transducer W is estimated as

$$W = \frac{\lambda^2 z^2 |p|^2}{2\pi \rho_0 c b^2} r^A \doteqdot 0.041. \tag{5}$$

If the number of the transducers used to form the array is N, the total radiation force F [N] that the ultrasound emitted from the array produces is

$$F = P \cdot N S_0 = \alpha \frac{w}{c} N S_0 = \alpha \frac{W}{c S_0} N S_0 = \alpha \frac{NW}{c}. \tag{6}$$

When N is 100 and α is 2, based on Eq. 6, the total radiation force is estimated as 2.4 [gf]. 2.4 gf is so small that it is difficult to perceive static pressure. However, it is expected that the radiation pressure can be modulated up to 1 kHz, which is sufficient bandwidth for human tactile perception and can induce perceivable vibratory sensation.

3   Prototype Device

We fabricated a prototype to confirm the feasibility of our method for producing tactile stimuli. The prototype consists of an annular array of airborne ultrasound transducers, a 12 channels amplifier circuit, and a PC. In order to measure the basic properties of acoustic radiation pressure produced with focused airborne ultrasound, the prototype was designed to produce a single focal point along the center axis perpendicular to the radiation surface.

3.1   Annular Array

Figure. 1 shows the annular array of airborne ultrasound transducers. The airborne ultrasound transducers (T4010A1, Nippon Ceramic) were packed in the

(a)   (b)

(c)
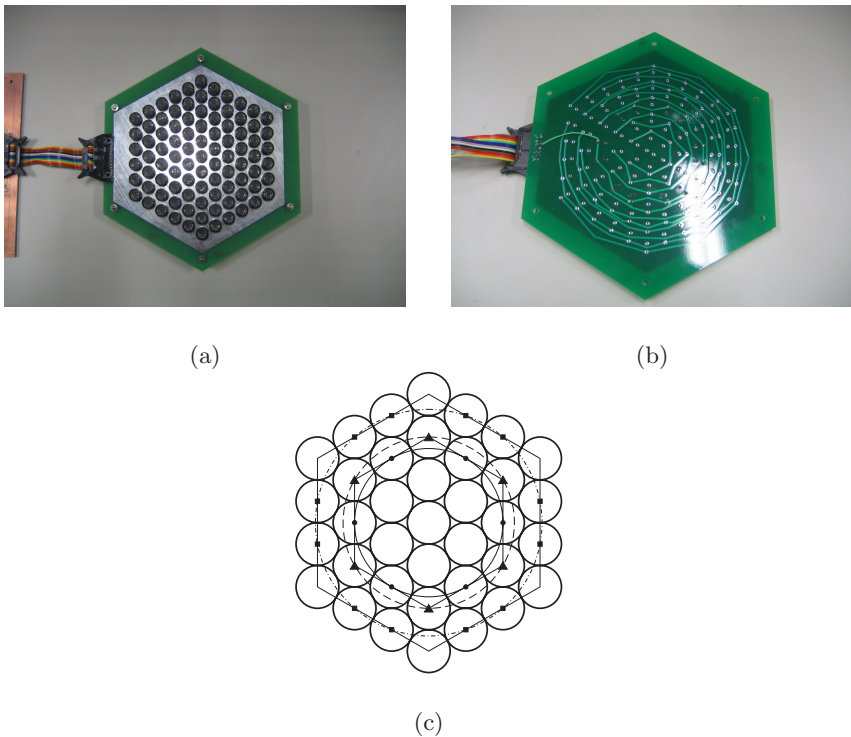
Fig. 1. Annular array of airborne ultrasound transducers. (a) The front side. It consists of 91 ultrasound transducers packed in the hexagonal arrangement. The diameter of each transducer is 1cm. (b) The back side. All of the transducers at the same distance from the center are electrically connected. (c) A schematic drawing to explain the electrical connection and arrangement of the transducers. The solid and dashed lines are the inscribed circle and the circumscribed circle of a hexagon, respectively. In these cases, 6 transducers are in the same distance from the center of the array. On the other hand, the number of the transducers on the dash-dot circle is 12.

hexagonal arrangement. The diameter of each transducer was 10 mm. The resonant frequency of the transducer was 40 kHz. The sound pressure emitted from the transducer is 20 Pa at 300 mm from the radiation surface.

The transducers which were in the same distance from the center of the array were connected to form a 12 channel annular array as in Fig. 1 (b). Fig. 1 (c) is the schematic drawing to explain the connection of the transducers. It is possible to draw three types of circles whose centers are at the center of the array as in Fig. 1 (c). If the circle is either the circumscribed or inscribed circle of a hexagon, the centers of 6 transducers are on the same circle. That means that the 6 transducers are in the same distance from the center of the array. The 6 transducers are electrically connected and driven at the same time. In case a circle and a hexagon have intersections, the number of the transducers in the same group is 12. Due to that arrangement, except for the transducer just at the center, each ring comprised of either 6 or 12 transducers.

The phase delay of the emitted ultrasound to the input signal is usually different among each transducer. Therefore, before fabricating the array, the phase delay was measured for each transducer and similar transducers were selected to form one ring.

3.2   System

Figure. 2 (a) shows the block diagram of the system. The system consists of a laptop PC with a digital I/O card (CSI292144, Interface Corporation), a 12 channel amplifier, and the annular array. Each channel of the digital I/O card output 40 kHz rectangular wave. The read-out rate for each channel of the digital I/O was 1 Mbps. Therefore, the time resolution of the phase delay was 1 μs. The outputs from the digital I/O were amplified with MOSFETs. The amplitude of the driving signal was 15 V.
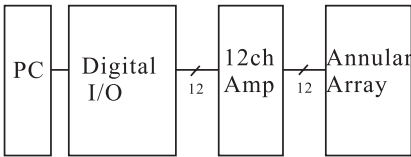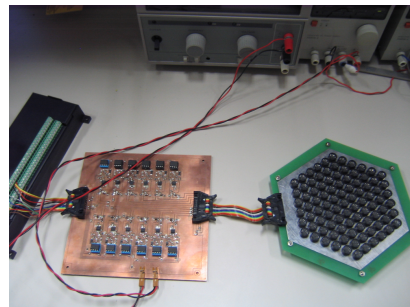
(a)   (b)

Fig. 2. (a) The block diagram of the prototype system (b) The driving circuit and the annular array. The driving circuit contains 12 channel amplifiers.

4   Evaluation

In order to confirm the feasibility of the prototype, the total force produced with the prototype, the spatial resolution of the radiation pressure and the frequency characteristics were measured. The subjective reports on tactile sensation are also described.

4.1   Total Force

The total force was measured using an electronic balance. The annular array was fixed just above the electronic balance placed on a table. The radiation surface of the array was faced toward the electronic balance. (i.e. the radiation surface was upside down.) The ultrasound was continuously radiated during the measurement. The focal point was fixed at 250 mm above the radiation surface and the distance between the radiation surface and the electronic balance was also fixed at 250 mm.The measured force was 0.8 gf when the amplitude of the input signal was 15 V. And in case the distance was 0 mm, the measured force was 2.9 gf, which is close to the theoretical value calculated in Section 2.

The measured force at the distance of 250 mm and 0 mm was different. The reason is that in the former case only the main lobe of the focused ultrasound was within the region of the top plate of the electronic balance and the sidelobe did not contribute to the total force. While in the latter case, all of the radiated ultrasound was applied on the top plate. Therefore, the force measured around the focal point will be improved by more efficient focusing method. We are now working on the simulation studies for confirming the effects on the efficiency caused by the array arrangement, the quantization of the driving signal, and so on.

4.2   Spatial Resolution

In order to measure the spatial distribution of the acoustic radiation pressure, we used a setup shown in Fig. 3. A microphone probe was attached to an XYZ stage. The accuracy of the position of the probe was 0.1 mm. The aperture of the microphone was ϕ 2 mm.

Figure. 4 (a) shows the spatial distribution of the acoustic radiation pressure along the x axis. The data were acquired at every 2 mm. The solid, dash-dot and dashed lines in Fig. 4 (a) correspond to the position of the focal point $z_f = 225$ mm, 250 mm and 275 mm, respectively.

Two features are seen in Fig. 4(a). First, the diameter of the focal point was about 20 mm regardless of the position of the focal point. Second, the maximum intensity decreases as the distance of the focal point from the array increases because of the attenuation of ultrasound in lossy medium.

4.3   Temporal Properties

Using the setup described in Section 4.2, the temporal properties of the radiation pressure were measured. The microphone was placed at the focal point. The focal

Microphone Probe

z

y

x

Annular Array

(a)   (b)
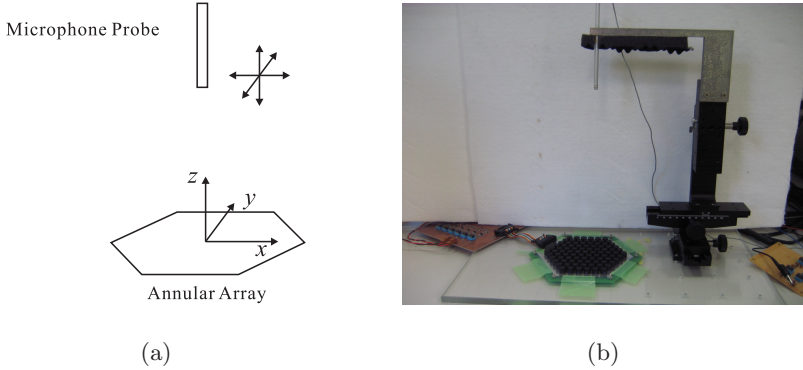
Fig. 3. Experimental setup for the measurement of the acoustic radiation pressure. (a): The XYZ coordinate was assigned as in the figure. A condenser microphone was attached to an XYZ stage. The aperture of the microphone was ϕ 2 mm. (b): The photograph of the setup.

point was fixed at z_f = 250 mm. The driving signal was 40 kHz rectangular wave modulated by burst wave of a particular frequency.

Figure. 5(a) shows the measured waveform of the radiation pressure. The modulation frequency was 80 Hz. The vertical axis represents the The horizontal axis represents time [ms]. As seen in the figure, the observed waveform was similar to a rectangular wave though it was not perfectly symmetric. It can be seen that there is a decrease of the radiation pressure starting from the onset of the radiation pressure during each half period. Fig. 5(b) shows the frequency characteristics of the radiation pressure. The horizontal axis represents the modulation frequency. The vertical axis represents the decibel gain of the amplitude of the radiation pressure. The decibel gain was set to 0 dB at 20 Hz. Note that in this measurement, the carrier frequency (the frequency of the ultrasound) was fixed at 40 kHz, but the sound power of the ultrasound was modulated by each frequency. The gain at 80 Hz, 1 kHz and 2 kHz were 3 dB, -4 dB and -12 dB, respectively.

4.4   Reports on Tactile Sensation

Several subjects tried the prototype and gave feedback on tactile sensation they felt. They clearly felt vibratory sensation when the radiation pressure was modulated by burst waves whose frequency was ranging from 20 Hz to 250 Hz. When constant radiation pressure was presented, they could feel only onset and offset of the radiation pressure. They also reported slight sensation of air flow just around the focal point. However the air flow was so weak that they could easily detect the position of the focal point. The cause of the air flow was considered to be the acoustic streaming.
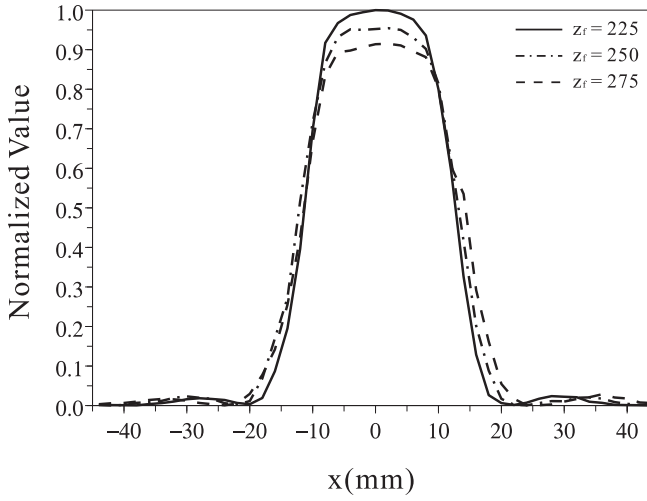
(a)
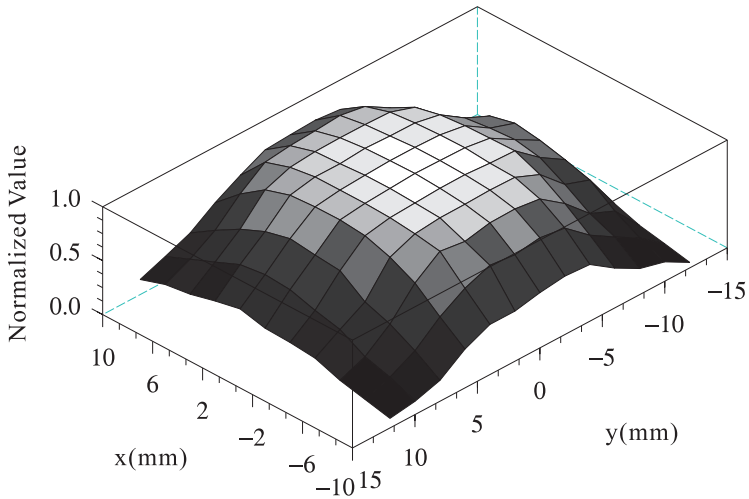
(b)

Fig. 4. Spatial distribution of the measured radiation pressure. The XY coordinates are the same as in Fig. 3. (a) A cross section along x-axis. The horizontal axis represents x axis. The vertical axis represents normalized value. The data for $z_f = 225$ mm, 250 mm and 275 mm are overlaid. (b) Two dimensional distribution of the radiation pressure around the focal point. The focal point was fixed at $z_f = 250$ mm in this case.

(a)   (b)
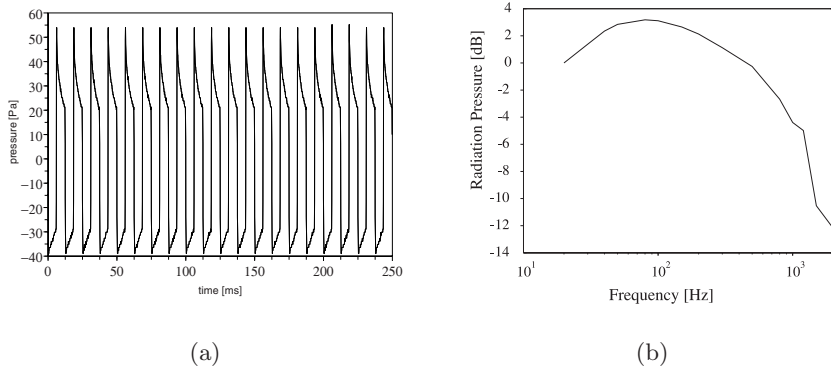
Fig. 5. Temporal properties of the measured radiation pressure. (a) The waveform of the radiation pressure measured at the focal point. The horizontal and vertical axes represent the time [ms] and the radiation pressure [Pa]. (b) The frequency characteristics for the radiation pressure. The horizontal axis represents the modulation frequency. The vertical axis represents the decibel gain. The decibel gain was set to 0 dB at 20 Hz.

5   Summary

In this paper, a tactile display using airborne ultrasound was presented. The prototype could produce 0.8 gf within the focal region. The spatial resolution was 20 mm. The prototype could produce sufficient vibrations up to 1 kHz. Though the produced force was weak for users to feel constant pressure, it was sufficient for vibratory sensation. Hence, the prototype is expected to be useful for providing tactile cues in accordance with contacting virtual objects, or for producing texture sensation. Now we are developing a 3D interaction system which enables its users to handle 3D graphic objects with tactile feedbacks without any gloves or wearable devices. We are also working on developing a complete 2D transducer array and its driver circuit.

References

1. Rodriguez, T., de Leon, A.C., Uzzan, B., Livet, N., Boyer, E., Geffray, F., Balogh, T., Megyesi, Z., Barsi, A.: Holographic and Action Capture Techniques. In: International Conference on Computer Graphics and Interactive Techniques (ACM SIGGRAPH 2007 emerging technologies) (2007)
2. Allard, J., Menier, C., Raffin, B., Boyer, E., Faure, F.: Grimage: Markerless 3D Interactions. In: International Conference on Computer Graphics and Interactive Techniques (ACM SIGGRAPH 2007 emerging technologies) (2007)
3. Immersion Corporation: CyberTouch, `http://www.immersion.com/`
4. Sato, K., Kajimoto, H., Kawakami, N., Tachi, S.: Electrotactile Display for Integration with Kinesthetic Display. In: Proceedings of the 16th IEEE International Conference on Robot and Human Interactive Communication (ROMAN 2007), pp. 3–8 (2007)

5. Suzuki, Y., Kobayashi, M.: Air Jet Driven Force Feedback in Virtual Reality. IEEE Computer Graphics and Applications 25(1), 44–47 (2005)
6. Drif, A., Citerin, J., Kheddar, A.: A Multilevel Haptic Display Design. In: Proceedings of 2004 IEE/RSJ International Conference on Intelligent Robots and Systems (IROS 2004), pp. 3595–3600 (2004)
7. Iwamoto, T., Shinoda, H.: Two-dimensional Scanning Tactile Display using Ultrasound Radiation Pressure. In: Proceedings of the Symposium on Haptic Interfaces for Virtual Environment and Teleoperator Systems (HAPTICS 2006) (2006)